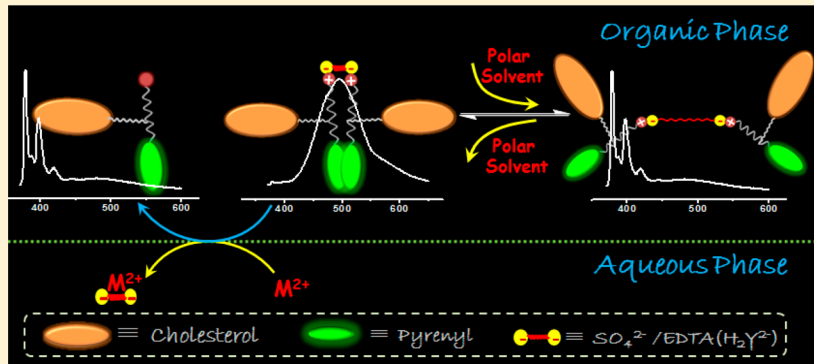


# Constitutional Dynamic Chemistry-based New Concept of Molecular Beacons for High Efficient Development of Fluorescent Probes

Xingmao Chang,<sup>†,‡</sup> Chunmeng Yu,<sup>†,§</sup> Gang Wang,<sup>†,§</sup> Jiayun Fan,<sup>†,§</sup> Jianyun Zhang,<sup>†,§</sup> Yanyu Qi,<sup>†,§</sup> Kaiqiang Liu,<sup>†,§</sup> and Yu Fang<sup>\*,†,‡,§</sup>

<sup>†</sup>Key Laboratory of Applied Surface and Colloid Chemistry (Ministry of Education), <sup>‡</sup>School of Materials Science and Engineering, and <sup>§</sup>School of Chemistry and Chemical Engineering, Shaanxi Normal University, Xi'an 710119, P. R. China

Supporting Information



**ABSTRACT:** Inspired by the concept of constitutional dynamic chemistry, we propose a new and well-adaptable strategy for developing molecular beacon (MB)-like fluorescent probes. To demonstrate the strategy, we synthesized and used an amino group containing pyrenyl derivative of cholesterol (CP) for the construction of new fluorescent probes with EDTA and sulfuric acid. The probes as created were successfully used for *n*-hexane purity checking and  $\text{Ba}^{2+}$  and  $\text{Pb}^{2+}$  sensing, respectively.

## 1. INTRODUCTION

Molecular beacons (MBs) are specifically designed fluorogenic DNA-based detection agents that were first reported in 1996.<sup>1</sup> Applications of MBs range from genetic screening, biosensor development, biochip construction, and the detection of single-nucleotide polymorphisms to mRNA monitoring in living cells.<sup>2–4</sup> Typically, MBs are dual-labeled with fluorophore and quencher groups at the 5' and 3' ends, respectively, and fold into a stem-loop or hairpin structure. It is the structure that holds the fluorophore and quencher units in close proximity to one another and results in fluorescence quenching.<sup>5–12</sup> Binding of a target, for example, a nucleic acid sequence complementary to the loop region, induces a conformational change, which opens the stem, separating the fluorophore and quencher units, and reactivates the fluorescence. Similarly, the two ends can be also labeled by same fluorophore moieties, of which the color of the light emitted depends on the loop structure.<sup>13–18</sup> The principle and ideas behind the design of MBs have been expanded and used to develop fluorescent probes with other functionalities.<sup>19–24</sup> For example, alkyls and alkoxy with calixarene, ionic binding, or other functional groups as side structures were employed as linkers of two relevant fluorophores. For example, pyrenyl motif was employed by Ding, Wallace, Wu, James, and Yoon for the creation of MB-like sensors, of which the sensors changed from a folded conformation to an extended one at the presence of suitable

targets, such as cations, anions, or neutral species including explosives.<sup>25–33</sup> In conjunction with the conformational change, the ratio of the excimer emission to the monomer emission also changes, a sign reporting on the recognition.

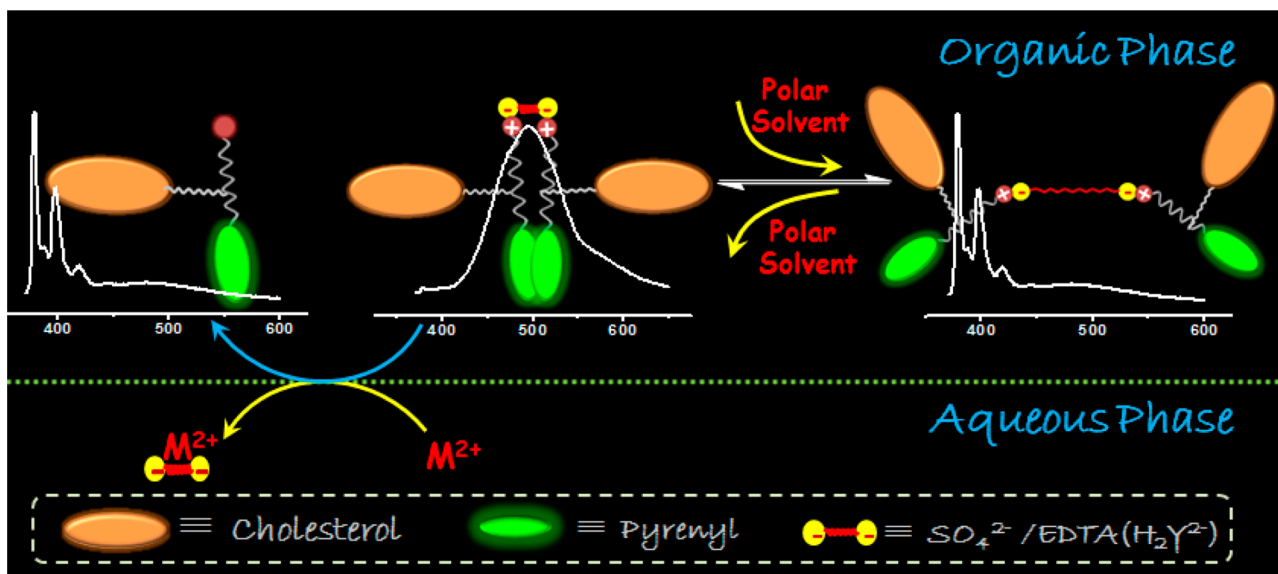
To the best of our knowledge, however, conventional MBs and the MB-like probes reported until now have been developed by covalent binding two relevant fluorophores or a fluorophore and a quencher, which may limit their applications due to tedious work in synthesis and simple in functionality. Therefore, the development of alternative strategies for creating MB-like sensors in a simple way and with multiple functionalities is of great importance. Inspired by the concept of constitutional dynamic chemistry (CDC) proposed by Lehn and others,<sup>34–41</sup> one strategy for realizing this envisagement is to design and prepare a suitable fluorescent structure containing a functional end group, such as proton-donating or -accepting unit; then, various MB-like sensors may be obtained by changing the linker in a physical way. Scheme 1 schematically shows the design of the MB-like fluorescent probes. The key to the design is the ionic association between the fluorophore derivative and the cross-linker with dual functionalities, which implies that the background fluorescence

Received: March 19, 2015

Revised: May 13, 2015

Published: May 18, 2015

Scheme 1. Cartoon Representing a New Strategy for Designing Constitutional Dynamic MB-Like Fluorescent Sensors and Their Possible Behaviors to the Presence of Polar Solvent or Metal Ions



will be characterized by pyrene excimer emission. Accumulation of polar molecules or binding of an analyte to the recognition domain (ionic region) extends or removes the linker and results in separation of the fluorophore moieties, allowing monomer emission. Thus, covalently binding of two relevant fluorophores or a fluorophore and a quencher is unnecessary.

Herein, we demonstrate the strategy with some examples, of which an amino-containing pyrenyl derivative (Py) of cholesterol (Chol) was taken as a main component (CP), which is characterized by a fluorescent Py unit, a hydrophobic Chol structure, and a proton acceptor amino group (cf. Figure 1). As examples, ethylene-diamine tetraacetic acid (EDTA) and sulfuric acid were used, separately, as a physical linker to combine two CPs together via proton transfer and resulted ion association. In this way, two different MB-like fluorescent probes, which are CP-EDTA and CP-SO<sub>4</sub>, respectively, were created. The probes as developed were successfully utilized for polarity sensing as well as Ba<sup>2+</sup> and Pb<sup>2+</sup> recognition.

## 2. EXPERIMENTAL SECTION

**2.1. Materials and Methods.** All intermediate compounds used were prepared by following procedures described in our previous publication.<sup>42,43</sup> Organic liquids used throughout were of analytical grade and used as received or dried to eliminate any water residue if necessary. Other reagents, except those specified, were of analytical grade and used without further purification. Water used in this work was acquired from a Milli-Q reference system.

Fluorescence measurements were performed at room temperature on a time-correlated single-photon counting fluorescence spectrometer (Edinburgh Instruments FLS 920). Time-resolved emission spectra (TRES) were measured on the same system using EPL-343 ps pulsed diode laser as an excitation source. The wavelength range of the TRES measurements was maintained from 370 to 652 nm. The monochromator was driven in a 3 nm step under the control of a computer. The accumulation time for each decay curve (a specific  $\lambda_{\text{ex}}/\lambda_{\text{em}}$ ) was 120 s. Transmission electron microscopy (TEM) image was obtained using Tecnai G2 F20 field

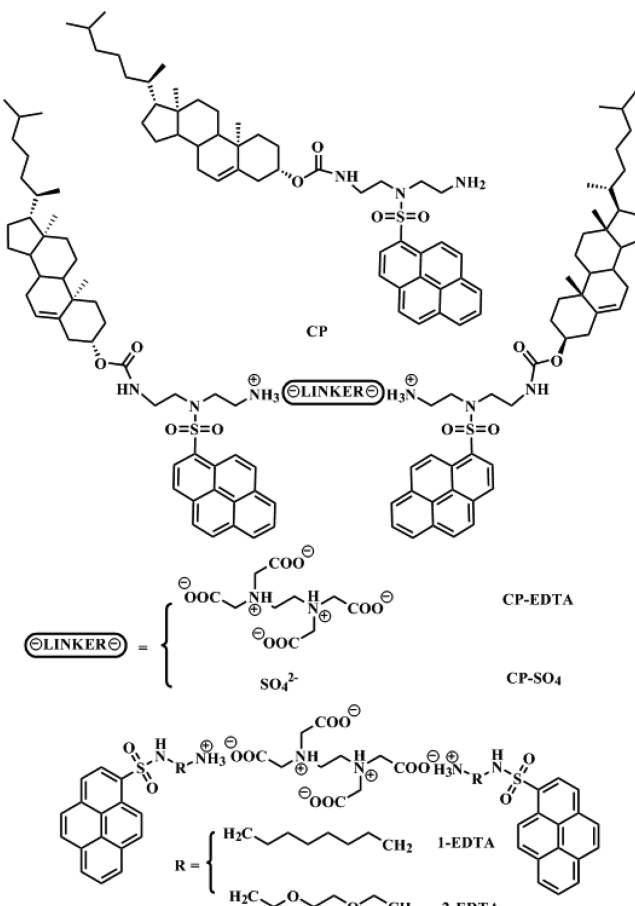


Figure 1. Structures of ionic associates.

transmission electron microscope at an acceleration voltage of 200 kV. Samples for TEM measurements were prepared by immersing a pure carbon-coated copper grid into chloroform and *n*-hexane solution of CP-EDTA ( $1.0 \times 10^{-6}$  mol/L), then the copper grid was removed from the solution, and then the solvent on its surface was evaporated completely at room

temperature. Determination of the particle size distribution and  $\zeta$  potential was performed on a Malvern Zetasizer Nano-ZS90.

**2.2. General Procedure for the Preparation of Ionic Associates.** One of the amine-terminated pyrenyl derivatives was dissolved in dry  $\text{CH}_2\text{Cl}_2$ ; then, the solution was added to the aqueous solution of a relevant acid. The stoichiometry of the two compounds was kept at 1:2 (mol to mol) so that theoretically protonation from carboxylic acid to organic amine is complete. The mixture was refluxed for 2 h to give an emulsion then cooled to room temperature; then, the solvents were evaporated. Finally, the ionic associates as obtained were further dried in vacuum. In this way, CP-EDTA, CP- $\text{SO}_4$ , and the two reference compounds, 1-EDTA and 2-EDTA, which are another two bis-pyrenyl derivatives but contain no cholesteryl residues, were prepared. The structures of the associates are shown in Figure 1.

### 3. RESULTS AND DISCUSSION

#### 3.1. Photophysical Behavior of CP-EDTA in Solution.

**3.1.1. Solvent Effect.** To reveal the polarity dependence of the fluorescence emission of the ionic associates, we took CP-EDTA as an example, and its fluorescence emission spectra were recorded in a variety of solvents including *n*-hexane, benzene, toluene, 1,4-dioxane, THF, chloroform, acetone, acetonitrile, and methanol at a concentration of  $1 \times 10^{-5}$  mol/L. The results are shown in Figure 2. Reference to the

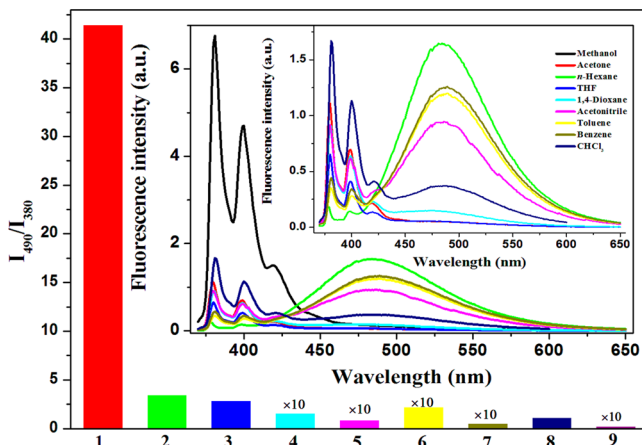


**Figure 2.**  $I_{490}/I_{380}$  of CP-EDTA recorded in different solvents: 1. *n*-hexane, 2. benzene, 3. toluene, 4. 1,4-dioxane, 5. THF, 6. chloroform, 7. acetone, 8. acetonitrile, and 9. methanol. Inset picture is fluorescence emission spectra of CP-EDTA in different solvents ( $1 \times 10^{-5}$  mol/L,  $\lambda_{\text{ex}} = 350$  nm), and for clarity, the inset shows the spectra with no methanol.

inset figure reveals that the profiles of the fluorescence emission in acetone, THF, and, in particular, methanol, is characterized by Py monomer emission, but in contrast in benzene, toluene, and, in particular, *n*-hexane, they are dominated by Py excimer emission. For other solvents, both emissions are seen. With quantitative analysis of the profiles of the spectra shown in the Figure, it was demonstrated that the ratio of  $I_{490}/I_{380}$  for *n*-hexane could be greater than 40, but for other solvents tested the ratio is <4; in particular, for methanol the ratio is close to 0. Further inspection of the spectra manifests that for all solvents studied the profile of the monomer emission part of the spectra recorded, including that from *n*-hexane is characterized by a low value of the  $I_3/I_1$  ratio, where  $I_1$  and  $I_3$  stand for the intensities

of peaks 1 and 3 of the emission, appearing at  $\sim 380$  and  $\sim 390$  nm, respectively, indicating a polar medium experienced by the Py units.<sup>44,45</sup> It is to be noted that the exact values of  $I_3$  are not clear due to absence of the peak, but it should be much lower than that of  $I_1$  due to weak emission at the position. Considering that some of the solvents, in particular, *n*-hexane, benzene, toluene, and so on, are highly hydrophobic but the immediate surroundings of the Py unit of the ionic associate experience a high polar medium, as indicated by the very low  $I_3/I_1$  values, it should be no doubt to conjecture that the Py unit is surrounded by ionic structures of the sensing compound. In other words, the molecules of CP-EDTA may exist in aggregated state.

**3.1.2. Concentration Effect and TRES Study.** To interrogate the origin of the fluorescence emission of CP-EDTA in the solvents, in particular, those of lower polarities, for example, *n*-hexane, toluene, and benzene, we conducted concentration-dependent fluorescence measurements, and the results are shown in Figure 3 and Figures S1 and S2 in the Supporting

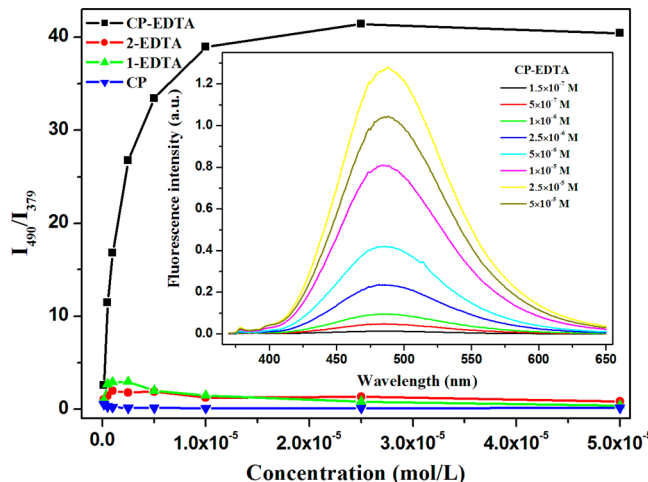


**Figure 3.** Plots of  $I_{490}/I_{380}$  against the concentration of the ionic associates in *n*-hexane. Inset shows the fluorescence emission spectra of CP-EDTA in *n*-hexane at different concentrations.

Information (SI), respectively. Taking *n*-hexane as an example, it is seen that within the concentration range studied, all of the spectra are dominated by Py excimer emission; however, the intensity ratio of the excimer emission to monomer emission ( $I_{490}/I_{380}$ ) increases dramatically along with increasing the concentration of the sensing compound at the beginning, but it does not change very much when the concentration exceeds  $1 \times 10^{-5}$  M, which could be a result of equilibrated structure or structure distribution of the aggregates of the compound. This is because further increase in the compound concentration could only result in increase in the number of the aggregates or the size of the aggregates, and both increases should have little effect on the excimer formation efficiency. This elaboration is further confirmed by TEM and DLS studies, as will be discussed later.

It is known that time-resolved emission spectroscopy (TRES) is a powerful technique to explore excited-state interactions of fluorescent compounds, and from the measurements one can have a better understand of the possible structures of the compound under study. Accordingly, the CP-EDTA/*n*-hexane system was studied by employing a TRES technique, and the results are shown in Figure 4. It is clearly

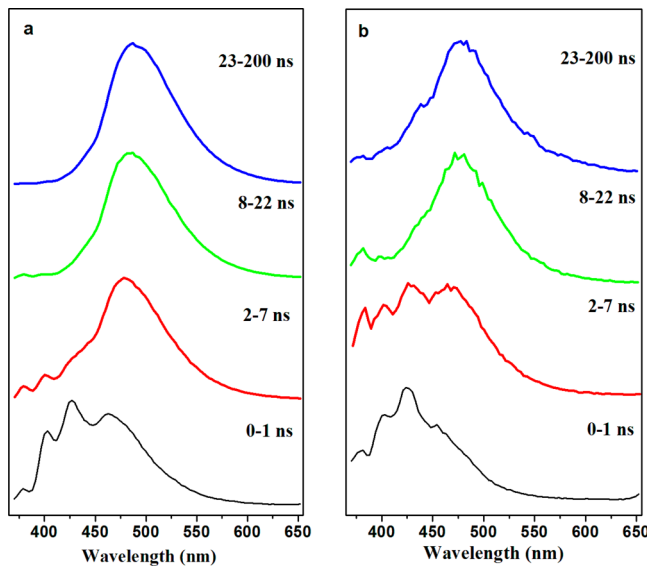
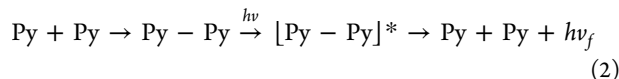
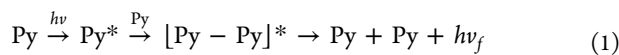


**Figure 4.** Time-resolved emission spectra of CP-EDTA in *n*-hexane, where a is the result from a concentration of  $1 \times 10^{-5}$  mol/L and b is the result from a concentration  $2 \times 10^{-7}$  mol/L.

seen that at a concentration of  $1 \times 10^{-5}$  M the profile of the earliest time gate (0–1 ns) spectrum is dominated by Py monomer and distorted Py excimer emission, which are characterized by weak emission before 400 nm and strong emission between 400 and 550 nm, respectively, but with the time gate moving to longer time (2–8 and 9–22 ns), the structure of the emission changes and the emission centering at 490 nm (the normal excimer) starts to dominate. In fact, for the spectra appearing in the time gates of 9–22 and 23–200 ns, emissions from the distorted excimer and monomer almost disappear, indicating clearly that in the solution studied Py excimer forms via both the preformed scheme and the Birks' scheme, as depicted in eqs 1 and 2, respectively.<sup>46,47</sup>



In other words, the Py units aggregated already before excitation, and in this case Py excimer forms via direct excitation of the ground-state dimer, the so-called preformed scheme (cf. eq 2). For the Birks' scheme, however, the situation is different. In this case, a Py unit in monomeric or free state is excited; then, it combines a ground-state Py unit in close proximity and forms an excited-state dimer (cf. eq 1). The excimer formed via the Birks' scheme emits in the same way as that formed via the preformed scheme. Functioning of preformed scheme is an indication of the presence of densely packed structure of the Py units, which could be either from a single molecule of CP-EDTA because it consists two Py units or from different molecules within a cluster of the compound. An additional TRES experiment in  $2 \times 10^{-7}$  mol/L confirmed that the preformed scheme is still functioning at so low concentration, suggesting that either CP-EDTA possesses a great tendency to form aggregates in *n*-hexane or structurally CP-EDTA adopts a collapsed conformation in the solvent due to presence of the ionic structure, which is highly incompatible with the medium. However, in conjunction with the appearance

of the preformed scheme, the Birks' scheme also functions, indicating that some of the Py units are mobile, which makes them have the ability to form excited-state dimer via rotational or translational motions. Anyway, no matter in which way the excimer formed, the fact that the fluorescence emission of the system is dominated by excimer emission is a strong evidence to reveal the aggregation of the compound in the solvent, even at concentrations lower than  $10^{-6}$  mol/L, as shown in the inset of Figure 3.

To have a deeper understanding of the results previously described, we also conducted concentration-dependent UV-vis spectroscopy measurements. The results are shown in Figure S3 in the SI. With reference to the spectra, it can be seen that in addition to the increase in the absorption intensity along with increasing concentration, the UV-vis spectra are all dominated by broad, less-structured absorptions positioning from 310 to 370 nm, which are typical absorptions of aggregate of pyrenyl units, no matter what the concentration of the system is, suggesting that the excimer emission may have mainly originated from direct excitation of the ground-state dimers of the fluorophore, a preformed scheme (cf. Figure 3), which is in agreement with the tentative conclusion from TRES studies (cf. Figure 4); furthermore, aggregation of pyrenyl moieties could be an intramolecular phenomenon. Comparison of the UV-vis spectra obtained in the present work with that of a conventional pyrene-based molecular beacon disclosed in a former report from our group<sup>25</sup> reveals the differences in the fluorescence behavior of present pyrene-based dynamic molecular beacon and that of the conventional one, of which the excimer originated mainly from Birks' scheme.

To explore if it is possible for CP-EDTA to form excimer in nonaggregated state and what kind of excimer will form if the answer to the first question is positive, we conducted additional fluorescence measurements of CP-EDTA in *n*-hexane at concentrations much lower than  $2 \times 10^{-7}$  mol/L, and the results are depicted in Figure 5. Study of the spectra shown in

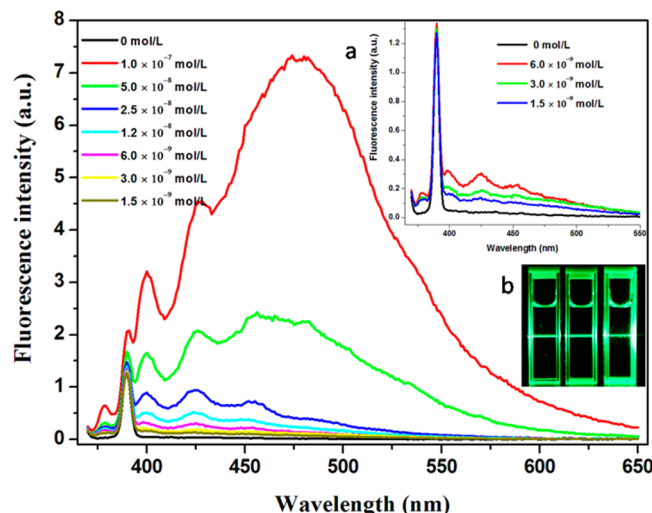


**Figure 5.** Fluorescence emission spectra of CP-EDTA in *n*-hexane at concentrations lower than  $1 \times 10^{-7}$  mol/L. Inset b is the spectra of the black and the spectra of three systems with lowest CP-EDTA concentrations, and that of b shows the Tyndall scattering pictures of CP-EDTA in *n*-hexane ( $5 \times 10^{-8}$  mol/L), pure *n*-hexane, and pure water (from left to right). Notice: The strong and sharp "emission" around 380 nm appearing in each system, including pure solvent, should be Raman scattering from the solvent.

the figure uncovers that with decreasing the concentration of the compound in the system the relative intensity of the excimer emission centering at  $\sim 490$  nm decreases, and at concentrations lower than  $5 \times 10^{-8}$  mol/L the emission is dominated by Py monomer and distorted Py excimer emission (cf. inset a' of Figure 5), suggesting that emission centering at  $\sim 490$  nm comes mainly from intermolecular interaction of the Py units, but distorted Py excimer emission could be from intramolecular interaction, as there is almost no aggregation at so low concentrations, which is confirmed by the absence of the scattering from Tynda II effect (cf. inset b' of Figure 5). It is to be noted that the strong and sharp "emission" around 380 nm appearing in each system, including pure solvent, under study should be Raman scattering from the solvent.<sup>3</sup>

Cholesterol (Chol) is a structure widely used as a building block for the creation of low-molecular-mass gelators due to its unique self-assembly property in various solvents; thereby, it is reasonable to speculate that the structure may have played an important role for the dissolution and aggregation of CP-EDTA in the systems studied. To get some information on the role of CP in the systems, we measured the concentration-dependent fluorescence emission spectra of two reference associates, 1-EDTA and 2-EDTA, which possess a similar core but different R structures with CP-EDTA, in *n*-hexane, and the results are shown in Figure S4 and Figure S5 (SI), respectively. With reference to the spectra and the  $I_{490}/I_{380}$  data shown in the Figures, it is observed that the values of the ratio of the two reference systems are less than 3 and do not change very much with increasing concentration, which is a result very different from that of CP-EDTA (cf. plots shown in Figure 3), suggesting a different solution behavior of the two compounds. As shown in Scheme 1, the two reference compounds possess a typical Py-based MB-like structure. Low excimer emission from the reference compounds is an indication that the Py moieties in the systems are relatively mobile. Far from that expected, the excimers formed in the two reference systems are also mainly coming from the preformed scheme, as confirmed by the corresponding TRES studies because the early time gate spectrum is dominated by both the monomer emission and the emission from the distorted excimers (cf. Figure S6, SI). This tentative conclusion is further confirmed by the profiles of the corresponding fluorescence decays obtained by monitoring them at both the monomer emission and the excimer emission regions (379 and 499 nm, respectively) (cf. Figure S7, SI). This is because with careful examination of the decays it is seen that there is no significant rising-up process in the peak region of each of the decays, which is an indication of functioning of the Birks' scheme. The time-resolved results previously discussed reveal that some of the Py units of the two reference compounds in the solution of the solvent exist in aggregated state, but others exist in monomer state. Of course, the aggregates should be dynamic, and exchange between them is highly possible. Further inspection of the emission spectra of the two references compounds (cf. Figures S4 and S5 in the SI, it is seen that the excimer emission from the system of 1-EDTA/*n*-hexane is more pronounced than that from 2-EDTA/*n*-hexane, suggesting R also plays an important role for the solution behavior of the dynamic bis-pyrenyl derivatives under study.

As another control, the concentration-dependent fluorescence emission of CP in *n*-hexane was studied, and the results are shown in Figure S8 (SI). At the same time, solvent effect on the emission of the compound was also tested, and the results

are depicted in Figure S9 (SI). With inspection of the Figures, it is clearly seen that for all of the systems studied, the emissions are all dominated by Py monomer emission; furthermore, the monomer emission is characterized by low  $I_3/I_1$  values, indicating the importance of Chol residues to the excimer-dominated emission behavior of CP-EDTA and the high polar medium experienced by the Py unit of the compound. Further inspection of the spectra reveals that compared with other solvents tested, *n*-hexane is a relatively poor solvent to the reference compound because from which a most obvious excimer emission is observed. This may explain why CP-EDTA shows a much more pronounced excimer emission in the solvent. All of the results from the control systems demonstrate that as an auxiliary unit or structure both Chol and EDTA have played an important role, and in fact they endowed the compound an extraordinary ability to make *n*-hexane be different from the others.

**3.2. Sensing Performance Studies.** **3.2.1. Purity Checking of *n*-Hexane.** Considering the fact that the  $E_T(30)^{48,49}$  value of *n*-hexane is very close to that of toluene, the big difference in the profiles of the fluorescence emission spectra of CP-EDTA recorded from *n*-hexane and toluene suggests that the MB-like probe developed in the present study may possess an extraordinary ability to verify the purity of the solvent.

It is well known that *n*-hexane is widely used as a solvent in the extraction of edible oil from soybean and other oilseeds, and it is also used as a denaturant and a cleaning agent in industry. Therefore, checking the purity of *n*-hexane in a reliable, simple, and fast way is important and challenging, particularly when the impurities are both physically and chemically inert.<sup>50</sup> Considering the fact that CP-EDTA possesses a distinct color in *n*-hexane within the solvents tested, it may be reasonable to study the feasibility if the compound could be used for checking the purity of *n*-hexane in a visualization way. Accordingly, the fluorescence emission of CP-EDTA in *n*-hexane was recorded in the presence of some other representative solvents, including CHCl<sub>3</sub>, benzene, and methanol, which are miscible with *n*-hexane within the composition range studied. First, the fluorescence emission spectra of the compound in a series of mixture solvents of *n*-hexane and chloroform were recorded, and the results are shown in Figure 6a. Clearly, as expected, the spectrum is characterized by Py monomer emission when the content of *n*-hexane in the mixture is <90% (v/v), but after that, emission from Py excimer starts to dominate the spectrum, as shown in the inset of the Figure. In other words, the presence of a small amount of other solvents in *n*-hexane would result in a great change in the profile of the fluorescence emission. Accordingly, a detailed study of the effect was performed, and the results are shown in Figure 6b and Figures S10 and S11 in the SI, respectively. It is seen that 33 ppm of the impurity solvents tested could result in a deduction of 3.3% of the maximum  $I_{490}/I_{380}$  value. Further treatment of the data obtained demonstrates that the detection limit of chloroform, benzene, and methanol in the solvent could be as low as 15 ppm, which is significantly lower than that required by national standard for food quality *n*-hexane.<sup>51</sup> The details of the DL calculation are provided in the SI.

**3.2.2. Sensing Mechanism.** The plausible mechanism of the sensing might be (1) the molecules of the probe, CP-EDTA, exist in aggregated state in *n*-hexane due to their ionic nature, (2) the molecules of the impurity (polar) solvents prefer to stay within the aggregates of the compound and result in extended

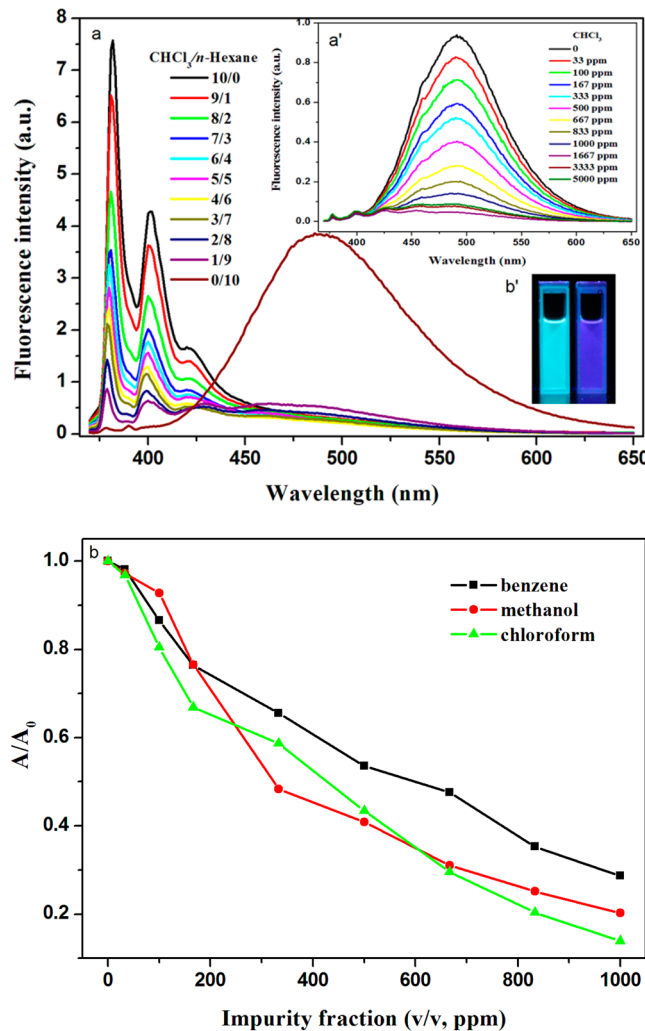


**Figure 6.** (a) Fluorescence emission spectra of CP-EDTA in CHCl<sub>3</sub>/ $n$ -hexane mixtures ( $1 \times 10^{-6}$  mol/L), the inset pictures: a' is a normalized result at the monomer position and b' is the picture of CP-EDTA in  $n$ -hexane (left) and mixture of  $n$ -hexane and CHCl<sub>3</sub>. (b) Plots of  $A/A_0$  as a function of the volume fraction of each impurity solvent in  $n$ -hexane ( $A = I_{490}/I_{380}$ ), where  $A_0$  stands for the ratio of the system with no impurity.

average size of the aggregates, and (3) it is the extension of the aggregates that may make the Py units away from each other and result in increased polarity of their microenvironment and corresponding decreasing in  $I_3/I_1$  values. This tentative argument is confirmed by the results from a number of experimental designs. TEM measurements revealed the aggregation of CP-EDTA in its  $n$ -hexane solution, and the average diameters of the aggregates vary from  $\sim 100$  to  $\sim 200$  nm at a concentration of  $1 \times 10^{-6}$  mol/L (cf. Figure 7a). Introduction of chloroform resulted in swelling or even fully disaggregation of the aggregates, as evidenced by TEM images shown in Figure 7b. In fact, further TEM measurements demonstrate that CP-EDTA is less aggregated in chloroform and in methanol (cf. Figure S12, SI), a result in support of the tentative conclusion depicted above. Of course, the aggregates observed in the TEM pictures might be formed during the evaporation of the solvents. To further examine the aggregation of the compound in the systems, we also conducted dynamic light scattering (DLS) measurements. Figure 7c depicts the result from CP-EDTA/ $n$ -hexane system study. It is seen that

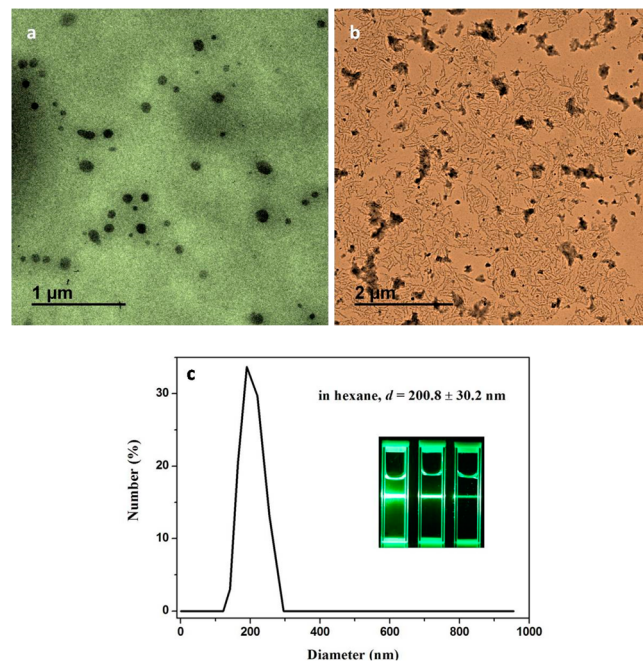


**Figure 7.** TEM images of the CP-EDTA aggregates from its  $n$ -hexane (a) and  $n$ -hexane/CHCl<sub>3</sub> (b) solutions ( $1.0 \times 10^{-6}$  mol/L), the corresponding particle size distribution from dynamic light scattering measurements (c), and Tyndall II scattering of CP-EDTA in  $n$ -hexane and methanol and pure water (from left to right) (inset picture of c).

the average diameter of the aggregates is  $\sim 200$  nm, a result reasonably larger than that obtained from TEM measurements,<sup>52</sup> but with the introduction of chloroform, the sizes of the aggregates increased, as evidenced by confusion of the light-scattering data. The reason behind might be that the original aggregates decomposed or dissolved into fibrous structures, as shown in the TEM images (cf. Figure 7b). The presence of aggregates in the CP-EDTA/ $n$ -hexane system was further confirmed by Tyndall II effect, as shown in Figure 7c (inset picture), but in contrast, the scattering in methanol is not obvious, a sign of less aggregation.

**3.3. Extension of the New Strategy.** It is to be noted that the strategy developed in the present study could be applied for the construction of other sensing structures. As an example, a Ba<sup>2+</sup> and Pb<sup>2+</sup> fluorescent probe was developed in a similar manner. As it is known, sulfate anion forms insoluble salts with the two cations in aqueous phase. Accordingly, H<sub>2</sub>SO<sub>4</sub> was used instead of EDTA to react with CP and result an ionic associate, CP-SO<sub>4</sub>, which should be a good sensor of the two cations. Figure S13 in the SI shows the fluorescence emission spectra of CP-SO<sub>4</sub> and that of CP in  $n$ -hexane. As expected, the emission of the associate is dominated by Py excimer emission, a sharp difference from that of CP, which is characterized by Py monomer emission. On the basis of this observation, the CP-SO<sub>4</sub>/ $n$ -hexane solution was used to identify Ba<sup>2+</sup> and Pb<sup>2+</sup> in aqueous phase. Figure 8 depicts the interaction results of a series of cations in aqueous phase with the CP-SO<sub>4</sub>/ $n$ -hexane solution. Clearly, the colors of the systems containing the two cations are different from the others, suggesting recognition of the two cations in a visualization way. Discrimination of the two cations is simple because the latter is dissolvable in concentrated sulfuric acid or sodium hydroxide.

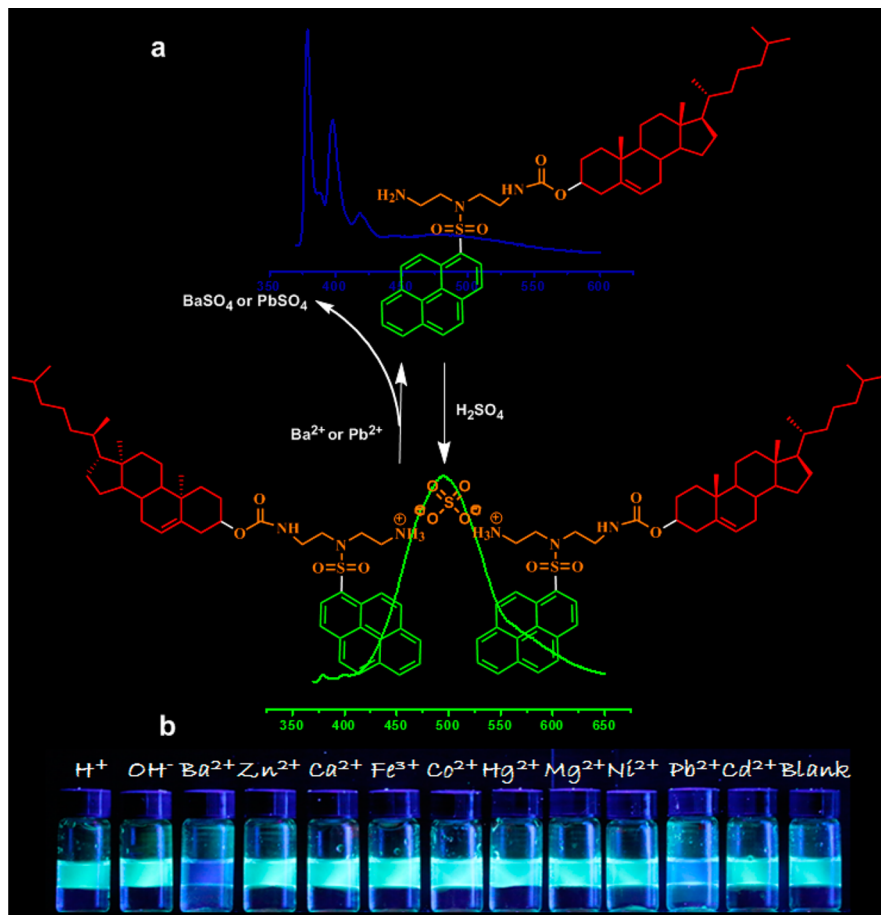


Figure 8. (a) Schematic representation of CP-SO<sub>4</sub> and CP with excimer–monomer switching. (b) Images of the mixtures of *n*-hexane solution of CP-SO<sub>4</sub> ( $1 \times 10^{-6}$  mol/L, upper layer) and aqueous solutions of relevant salts or acid or base ( $1 \times 10^{-6}$  mol/L, bottom layer) under UV light.

## 4. CONCLUSIONS

In conclusion, we have developed a new strategy for developing MB-like fluorescence sensors via construction of simple fluorescent ionic associates. The main difference between our sensors and those of conventional MBs is the constitutional dynamic nature of our sensors that is partial of the linkers of our sensors could be extended or removed during sensing, a property very different from the change of rigidity of conventional MBs during sensing. Another key point of our sensors is the introduction of auxiliary unit, Chol, which promotes the formation of excimer structures when Py was adopted as a sensing fluorophore, a basis for sensing. This conceptual design was verified by two example systems, CP-EDTA, and CP-SO<sub>4</sub>. The main limitation of the sensors presented might be their sensing at interfaces, which makes utilization of organic solvent unavoidable. Therefore, development of biocompatible, aqueous phase-only MB-like sensors is one of the main concerns of our future research. Anyway, we believe that our strategy is of great importance for developing a new generation of fluorescence sensors.

## ■ ASSOCIATED CONTENT

### Supporting Information

The details of the determination and calculation of the detection limits (DLs), some fluorescence spectra, TRES, fluorescence decays, and TEM images. The Supporting Information is available free of charge on the ACS Publications website at DOI: 10.1021/acs.jpcb.5b02664.

## ■ AUTHOR INFORMATION

### Corresponding Author

\*E-mail: yfang@snnu.edu.cn. Tel: 0086-29-81530786. Fax: 0086-29-81530787.

### Notes

The authors declare no competing financial interest.

## ■ ACKNOWLEDGMENTS

This work was supported by the Natural Science Foundation of China (21273141), the 111 project (B14041), and the Program for Changjiang Scholars and Innovative Research Team in University (IRT1070). This work was also supported by Research Funds of Shaanxi Normal University (X2014YB04).

## ■ REFERENCES

- Tyagi, S.; Kramer, F. R. Molecular Beacons: Probes that Fluoresce upon Hybridization. *Nat. Biotechnol.* **1996**, *14*, 303–308.
- Yang, C. J.; Tan, W. H. *Molecular Beacons*; Springer-Verlag: Berlin, 2013.
- Lakowicz, J. R. *Principles of Fluorescence Spectroscopy*, 3rd ed.; Springer Science & Business Media: New York, 2006.
- Demchenko, A. P. *Introduction to Fluorescence Sensing*; Springer Science & Business Media: London, 2009.
- Tyagi, S. Imaging Intracellular RNA Distribution and Dynamics in Living Cells. *Nat. Methods* **2009**, *6*, 331–338.
- Tyagi, S.; Bratu, D. P.; Kramer, F. R. Multicolor Molecular Beacons for Allele Discrimination. *Nat. Biotechnol.* **1998**, *16*, 49–53.

- (7) Ortiz, E.; Estrada, G.; Lizardi, P. M. PNA Molecular Beacons for Rapid Detection of PCR Amplicons. *Mol. Cell. Probes* **1998**, *12*, 219–226.
- (8) Drake, T. J.; Tan, W. H. Molecular Beacon DNA Probes and their Bioanalytical Applications. *Appl. Spectrosc.* **2004**, *58*, 269A–280A.
- (9) Kostrikis, L. G.; Tyagi, S.; Mhlanga, M. M.; Ho, D. D.; Kramer, F. R. Spectral Genotyping of Human Alleles. *Science* **1998**, *279*, 1228–1229.
- (10) Wang, K. M.; Tang, Z. W.; Yang, C. J.; Kim, Y.; Fang, X. H.; Li, W.; Wu, Y. R.; Medley, C. D.; Cao, Z. H.; Li, J.; et al. Molecular Engineering of DNA: Molecular Beacons. *Angew. Chem., Int. Ed.* **2009**, *48*, 856–870.
- (11) Li, Y. S.; Zhou, X. Y.; Ye, D. Y. Molecular Beacons: An Optimal Multifunctional Biological Probe. *Biochem. Biophys. Res. Commun.* **2008**, *373*, 457–461.
- (12) Goel, G.; Kumar, A.; Puniya, A. K.; Chen, W.; Singh, K. Molecular Beacon: A Multitask Probe. *J. Appl. Microbiol.* **2005**, *99*, 435–442.
- (13) Østergaard, M. E.; Hrdlicka, P. J. Pyrene-Functionalized Oligonucleotides and Locked Nucleic Acids (LNAs): Tools for Fundamental Research, Diagnostics, and Nanotechnology. *Chem. Soc. Rev.* **2011**, *40*, 5771–5788.
- (14) Lee, M. H.; Kim, J. S.; Sessler, J. L. Small Molecule-Based Ratiometric Fluorescence Probes for Cations, Anions, and Biomolecules. *Chem. Soc. Rev.* **2015**, DOI: 10.1039/c4cs00280f.
- (15) Bains, G.; Patel, A. B.; Narayanaswami, V. Pyrene: A Probe to Study Protein Conformation and Conformational Changes. *Molecules* **2011**, *16*, 7909–7935.
- (16) Wu, J. C.; Zou, Y.; Li, C. Y.; Sicking, W.; Piantanida, I.; Yi, T.; Schmuck, C. A Molecular Peptide Beacon for the Ratiometric Sensing of Nucleic Acids. *J. Am. Chem. Soc.* **2012**, *134*, 1958–1961.
- (17) Fujimoto, K.; Mutoa, Y.; Inouye, M. A General and Versatile Molecular Design for Host Molecules Working in Water: A Duplex-Based Potassium Sensor Consisting of Three Functional Regions. *Chem. Commun.* **2005**, 4780–4782.
- (18) Fujimoto, K.; Yamada, S.; Inouye, M. Synthesis of Versatile Fluorescent Sensors Based on Click Chemistry: Detection of Unsaturated Fatty Acids by their Pyrene-Emission Switching. *Chem. Commun.* **2009**, 7164–7166.
- (19) Blackstock, D.; Chen, W. Halo-Tag Mediated Self-labeling of Fluorescent Proteins to Molecular Beacons for Nucleic Acid Detection. *Chem. Commun.* **2014**, *50*, 13735–13738.
- (20) Ding, L. P.; Fang, Y. Chemically Assembled Monolayers of Fluorophores as Chemical Sensing Materials. *Chem. Soc. Rev.* **2010**, *39*, 4258–4273.
- (21) Lau, Y. H.; Rutledge, P. J.; Watkinson, M.; Todd, M. H. Chemical Sensors that Incorporate Click-derived Triazoles. *Chem. Soc. Rev.* **2011**, *40*, 2848–2866.
- (22) Kim, H. N.; Ren, W. X.; Kim, J. S.; Yoon, J. Fluorescent and Colorimetric Sensors for Detection of Lead, Cadmium, and Mercury Ions. *Chem. Soc. Rev.* **2012**, *41*, 3210–3244.
- (23) Moragues, M. E.; Martínez-Máñez, R.; Sancenón, F. Chromogenic and Fluorogenic Chemosensors and Reagents for Anions. A Comprehensive Review of the Year 2009. *Chem. Soc. Rev.* **2011**, *40*, 2593–2643.
- (24) Santos-Figueroa, L. E.; Moragues, M. E.; Climent, E.; Agostini, A.; Martínez-Máñez, R.; Sancenón, F. Chromogenic and Fluorogenic Chemosensors and Reagents for Anions. A Comprehensive Review of the Years 2010–2011. *Chem. Soc. Rev.* **2013**, *42*, 3489–3613.
- (25) Wang, S. H.; Ding, L. P.; Fan, J. M.; Wang, Z. X.; Fang, Y. Bispyrene/Surfactant-Assembly-Based Fluorescent Sensor Array for Discriminating Lanthanide Ions in Aqueous Solution. *ACS Appl. Mater. Interfaces* **2014**, *6*, 16156–16165.
- (26) Ding, L. P.; Wang, S. H.; Liu, Y.; Cao, J. H.; Fang, Y. Bispyrene/Surfactant Assemblies as Fluorescent Sensor Platform: Detection and Identification of Cu<sup>2+</sup> and Co<sup>2+</sup> in Aqueous Solution. *J. Mater. Chem. A* **2013**, *1*, 8866–8875.
- (27) Cao, Y.; Ding, L. P.; Hu, W. T.; Peng, J. X.; Fang, Y. A Surfactant-Modulated Fluorescent Sensor with Pattern Recognition Capability: Sensing and Discriminating Multiple Heavy Metal Ions in Aqueous Solution. *J. Mater. Chem. A* **2014**, *2*, 18488–18496.
- (28) Ding, L. P.; Bai, Y. M.; Cao, Y.; Ren, G. J.; Blanchard, G. J.; Fang, Y. Micelle-Induced Versatile Sensing Behavior of Bispyrene-based Fluorescent Molecular Sensor for Picric Acid and PYX Explosives. *Langmuir* **2014**, *30*, 7645–7653.
- (29) Manandhar, E.; Broome, J. H.; Myrick, J.; Lagrone, W.; Cragg, P. J.; Wallace, K. J. A Pyrene-based Fluorescent Sensor for Zn<sup>2+</sup>Ions: A Molecular ‘Butterfly’. *Chem. Commun.* **2011**, *47*, 8796–8798.
- (30) Ma, B. L.; Zeng, F.; Li, X. Z.; Wu, S. Z. A Facile Approach for Sensitive, Reversible and Ratiometric Detection of Biothiols Based on Thymine-Mediated Excimer-Monomer Transformation. *Chem. Commun.* **2012**, *48*, 6007–6009.
- (31) Kim, S. K.; Lee, S. H.; Lee, J. Y.; Lee, J. Y.; Bartsch, R. A.; Kim, J. S. An Excimer-based, Binuclear, On-Off Switchable Calix[4]crown Chemosensor. *J. Am. Chem. Soc.* **2004**, *126*, 16499–16506.
- (32) Xu, Z. C.; Singh, N. J.; Lim, J.; Pan, J.; Kim, H. N.; Park, S.; Kim, K. S.; Yoon, J. Unique Sandwich Stacking of Pyrene-Adenine-Pyrene for Selective and Ratiometric Fluorescent Sensing of ATP at Physiological pH. *J. Am. Chem. Soc.* **2009**, *131*, 15528–15533.
- (33) Phillips, M. D.; Fyles, T. M.; Barwell, N. P.; James, T. D. Carbohydrate Sensing Using a Fluorescent Molecular Tweezer. *Chem. Commun.* **2009**, 6557–6559.
- (34) Lehn, J.-M. Perspectives in Chemistry—Steps Towards Complex Matter. *Angew. Chem., Int. Ed.* **2013**, *52*, 2836–2850.
- (35) Lehn, J.-M. Perspectives in Chemistry—Aspects of Adaptive Chemistry and Materials. *Angew. Chem., Int. Ed.* **2015**, *54*, 3276–3289.
- (36) Lehn, J.-M. From Supramolecular Chemistry towards Constitutional Dynamic Chemistry and Adaptive Chemistry. *Chem. Soc. Rev.* **2007**, *36*, 151–160.
- (37) Legrand, Y.-M.; Dumitru, F.; Arnal-Herault, C.; Michau, M.; Barboiu, M. D. Dynamic Constitutional materials. Crystallization- and Sol-Gel-Driven Self-sorting of Functional Supramolecular Architectures. *Rev. Roum. Chim.* **2009**, *54*, 421–432.
- (38) Jin, Y. H.; Yu, C.; Denman, R. J.; Zhang, W. Recent Advances in Dynamic Covalent Chemistry. *Chem. Soc. Rev.* **2013**, *42*, 6634–6654.
- (39) Rowan, S. J.; Cantrill, S. J.; Cousins, G. R. L.; Sanders, J. K. M.; Stoddart, J. F. Dynamic Covalent Chemistry. *Angew. Chem., Int. Ed.* **2002**, *41*, 898–952.
- (40) Corbett, P. T.; Leclaire, J.; Vial, L.; West, K. R.; Wietor, J.-L.; Sanders, J. K. M.; Otto, S. Dynamic Combinatorial Chemistry. *Chem. Rev.* **2006**, *106*, 3652–3711.
- (41) Reek, J. N. H.; Otto, S. *Dynamic Combinatorial Chemistry*; Wiley-VCH: Weinheim, Germany, 2010.
- (42) Chang, X. M.; Wang, G.; Yu, C. M.; Wang, Y. R.; He, M. X.; Fan, J.; Fang, Y. Studies on the Photochemical Stabilities of Some Fluorescent Films Based on Pyrene and Pyrenyl Derivatives. *J. Photochem. Photobiol. A* **2015**, *298*, 9–16.
- (43) Wang, G.; Chang, X. M.; Peng, J. X.; Liu, K. Q.; Zhao, K. R.; Yu, C. M.; Fang, Y. Towards a New FRET System via Combination of Pyrene and Perylene Bisimide: Synthesis, Self-Assembly and Fluorescence Behavior. *Phys. Chem. Chem. Phys.* **2015**, *17*, 5441–5449.
- (44) Dong, D. C.; Winnik, M. A. The Py Scale of Solvent Polarities. Solvent Effects on the Vibronic Fine Structure of Pyrene Fluorescence and Empirical Correlations with  $E_T$  and Y Values. *Photochem. Photobiol.* **1982**, *35*, 17–21.
- (45) Dong, D. C.; Winnik, M. A. The Py Scale of Solvent Polarities. *Can. J. Chem.* **1984**, *62*, 2560–2565.
- (46) Birks, J. B. Excimers and Exciplexes. *Nature* **1967**, *214*, 1187–1190.
- (47) Birks, J. B. Excimers. *Rep. Prog. Phys.* **1975**, *38*, 903–974.
- (48) Reichardt, C. Solvatochromic Dyes as Solvent Polarity Indicators. *Chem. Rev.* **1994**, *94*, 2319–2358.
- (49) Zhao, K. R.; Liu, T. H.; Wang, G.; Chang, X. M.; Xue, D.; Belfield, K. D.; Fang, Y. A Butterfly-shaped Pyrene Derivative of Cholesterol and Its Uses as a Fluorescent Probe. *J. Phys. Chem. B* **2013**, *117*, 5659–5667.
- (50) Hui, Y. H. *Bailey's Industrial Oil and Fat Product*, 5th ed.; John Wiley & Sons, Inc.: New York, Vol. 4, 2001.

(S1) Emmandi, R.; Sastry, M. I. S.; Patel, M. B. Low Level Detection of Benzene in Food Grade Hexane by Ultraviolet Spectrophotometry. *Food Chem.* **2014**, *161*, 181–184.

(S2) Takashi, I.; Li, S.; Michael, A. B.; Richard, M. C. Comparison of Nanoparticle Size and Electrophoretic Mobility Measurements Using a Carbon-Nanotube-Based Coulter Counter, Dynamic Light Scattering, Transmission Electron Microscopy, and Phase Analysis Light Scattering. *Langmuir* **2004**, *20*, 6940–6945.